NASA

Technical Memorandum **80565**

Interplanetary Sector Boundaries 1971 - 1973

L. Klein and L. F. Burlaga

(NASA-TM-80565) INTERPLANETARY SECTOR BOUNDARIES, 1971 - 1973 (NASA) 35 p HC A03/MF A01 CSCL 03B
N79-34133
Unclas
G3/90 38909

SEPTEMBER 1979

National Aeronautics and
Space Administration

Goddard Space Flight Center
Greenbelt, Maryland 20771

INTERPLANETARY SECTOR BOUNDARIES

1971-1973

by

L. Klein
L. F. Burlaga
NASA/Goddard Space Flight Center
Laboratory for Extraterrestrial Physics
Greenbelt, MD 20771

To be submitted to: JOURNAL OF GEOPHYSICAL RESEARCH

ABSTRACT

Eighteen interplanetary sector boundary crossings observed at 1 AU during the period January 1971 to January 1974 by the magnetometer on the IMP-6 spacecraft are discussed. The events were examined on many different time scales ranging from days on either side of the boundary to high resolution measurements of 12.5 vectors per second. Two categories of boundaries were found, one group being relatively thin (averaging $\backsim 10^4$ km), and the other being thick (averaging $\backsim 10^5$ km). In many cases the field vector rotated in a plane from one polarity to the other. Only two of the transitions were null sheets. Using the minimum variance analysis to determine the normals to the plane of rotation, and assuming that this is the same as the normal to the sector boundary surface, it was found that the normals were close to ($\lesssim 45°$) the ecliptic plane. The high inclination of the sector boundary surfaces during 1971-1973 may be related to the presence of large equatorial coronal holes at this time. An analysis of tangential discontinuities contained in 4-day periods about our events showed that their orientations were generally not related to the orientations of the sector boundary surface, but rather their characteristics were about the same as those for discontinuities outside the sector boundaries. Magnetic holes were found in thick sector boundaries, at a rate about three times that elsewhere. The holes were especially prevalent near stream interfaces, suggesting that they might be related to the convergence and/or slip of adjacent solar wind streams.

1. Introduction

Interplanetary sectors are extended regions in which the interplanetary magnetic field is directed primarily away from (or toward) the sun. Sectors have been studied extensively since their discovery by Wilcox and Ness (1965). The boundaries between sectors are often relatively distinct in plots of the magnetic field direction for intervals of $\lesssim$ 27 days, and perhaps for this reason sector boundaries have been correlated with many solar-terrestrial phenomena. For example, they have been correlated with solar features and interplanetary streams (Ness and Wilcox, 1964; and see Hundhausen, 1972, 1977), with geomagnetic activity (Wilcox, 1968), and even with weather systems (Wilcox et al., 1974, Svalgaard, 1976). These studies have shown that the sector boundaries and sector structure often provide a means of organizing solar-terrestrial data, even though the reason for this is not always clear. In order to understand the origin of sector boundaries and the relations between sector boundaries and other phenomena, it is important to learn more about the nature, morphology and internal structure of sector boundaries. That is the aim of this work.

The morphology, especially the latitudinal extent, of sector boundaries has been discussed in several papers, with a variety of results. Wilcox and Svalgaard (1974) suggested that the surfaces of sector boundaries might be oriented perpendicular to the solar equatorial plane; Rosenberg and Coleman (1969), Rosenberg (1970, 1975), Fairfield and Ness (1974), Behannon and Neubauer (1979), and Behannon et al. (1979) presented evidence that sector boundary surfaces might lie close to the ecliptic plane; Svalgaard et al.(1974) showed how intermediate inclinations might be obtained; and Schulz (1973), Levy (1976), and Alfvén (1977) argued theoretically that the sector boundary surface might lie near the solar equatorial plane on average. Recent indirect evidence for the shape of sector boundaries, based on measurements of the sector structure and on coronal holes and open magnetic field lines at the sun (Hundhausen, 1977; Burlaga et al., 1978), tends to support the Schulz-Levy-Alfvén picture. Burlaga et al. (1978) pointed out that a variety of shapes and orientations is possible, depending on the relative positions of coronal holes which produce the streams that contain sectors. (Stationary interplanetary streams are generally unipolar, and sector boundaries always occur between streams.)

Thus, the morphology of the sector boundary surface might change with solar activity. Measurements have recently been made of the latitudinal variations of the sector boundary surface in 1976. Pioneer 11 observations obtained at 3.7-5 AU, showed that the sector structure disappeared at 16° above the ecliptic and positive sectors became increasingly dominant as the spacecraft moved to higher latitudes (Smith et al., 1978). Helios 1 and 2 observations obtained between 1 AU and 0.3 AU, determined the latitudes of recurrent sector boundary crossings as a function of longitude for four solar rotations, giving a direct measurement of the shape of a sector boundary surface (Villante et al., 1979). Both the Pioneer 11 and Helios results are consistent with a warped current sheet inclined $\backsim$ 10° to 15° with respect to the solar equator. In this paper (section 3) we investigate the orientation of sector boundaries in the period 1971-1973, using data on the internal structure of sector boundaries obtained at 1 AU. We find higher inclinations than observed in 1976, suggesting a possible solar cycle variation.

The internal structure of sector boundaries has been found to be very complex (Behannon and Neubauer, 1979). We observed similar complexity and found no uniform way to describe it. We consider only two of the phenomena which are found inside of sector boundaries--directional discontinuities and magnetic holes. We investigated directional discontinuities (section 4) in the hope that they might provide information on the orientation of sector boundary surfaces, but the results were negative for the set of discontinuities that we considered. Magnetic holes were considered (section 5) because they are a prominent feature in sector boundaries; the results do not, however, support the widely-held view that sector boundaries are null sheets.

2. Selection and Classification of Sector Boundaries

For this study, we define a sector boundary (hereafter designated SB) as a transition between two sectors, each sector being a nearly unipolar region in which the magnetic field is close to the spiral direction and which passes the earth in 2 days or more. Sector boundaries were identified in 27-day plots of hour averages of $\mathbf{B}$, compiled by King (1977). The only restriction on the thickness was that the transition should occur in significantly less than 2 days. We excluded intervals containing shock waves, to avoid flare-associated flow configurations and any other such transients. We also required that the data coverage in the 4-day interval containing the SB should be nearly complete.

Eighteen sector boundaries were selected in the 3-year interval that was examined (January, 1971 to January, 1974). This is only a fraction (approximately 1/4 to 1/8) of all the SBs that were present but it is probably a representative sample. The size of our sample is limited, primarily because 1) we considered only periods for which we have IMP-6 observations (IMP-6 is in the solar wind only $\approx$ 6 months/yr), 2) we required fairly continuous magnetic field coverage in the 4-day interval containing each sector boundary, and 3) we required that plasma data should be available for the intervals selected.

Throughout this paper, $\underset{\sim}{B}$ is measured in solar ecliptic coordinates. The azimuthal direction (ϕ) is measured in the ecliptic plane, increasing counter-clockwise as seen by an observer north of the ecliptic; it is zero when $\underset{\sim}{B}$ points toward the sun. The inclination of $\underset{\sim}{B}$ with respect to the ecliptic plane (θ) is positive when $\underset{\sim}{B}$ points above the plane.

Figure 1 shows the distribution of ϕ angles before and after the SBs that were selected for this study. This and Figure 7 (to be discussed later) confirm that the magnetic field was predominantly along the spiral direction and that the polarity of $\underset{\sim}{B}$ reversed across the chosen boundaries. Also shown in Figure 1 are the distributions of the magnetic field intensity and the variance (σ) in the Cartesian components of $\underset{\sim}{B}$ over 1-hr intervals. The distributions of B and σ are significantly broader after the SB than before. This is because SBs are usually followed by interaction regions, where the intensity and fluctuations in $\underset{\sim}{B}$ are generally higher than average.

The high resolution magnetic field data (up to 12.5 vectors/s) that were used in our study of the structure of SBs were obtained by the NASA/GSFC magnetometer on IMP-6. The principal investigator of that experiment is N. F. Ness. A description of the instrument was presented by Fairfield (1974). The high sampling rates of the IMP-6 magnetometer resolved structures with scales smaller than the thermal ion gyroradius; thus, all of the important magnetic field characteristics of SBs were clearly resolved.

Let us now consider specific examples of sector boundaries and show how they can be classified. Figure 2 shows a SB on January 6,1973; the data are 12.5 averages of $\underset{\sim}{B}$. There are 4 significant characteristics of this SB. First, the transition occurs in less than 10 min. This is an example of one class of sector boundaries which we refer to as "thin" boundaries. Second, the magnetic field intensity does not go to zero while the magnetic field changes direction, i.e., the SB is not a null sheet. The magnetic field direction changes by means of a rotation of $\underset{\sim}{B}$ rather than by $|\underset{\sim}{B}|$ shrinking to zero along a fixed direction. Third, the field moves out of the ecliptic (high values of $|\theta|$) during the sector transition. Fourth, the reversal of $\underset{\sim}{B}$ occurs by means of a rotation in a plane, i.e., the structure of the SB resembled that of a tangential discontinuity. The large values of $|\theta|$ in the transition imply that the rotation plane was highly inclined with respect to the ecliptic.

We used the standard minimum variance technique (Sonnerup and Cahill, 1967) to analyze the change in $\underset{\sim}{B}$ across a SB (see Lepping and Behannon, (1979), Burlaga et al., 1977, and the references therein for a discussion of this method). Basically, the technique determines a plane which best fits the vectors $\underset{\sim}{B}_i - \langle \underset{\sim}{B} \rangle$, where $\langle \underset{\sim}{B} \rangle$ is the average field in the transition, and $\underset{\sim}{B}_i$ are the measured values. The normal to this plane $(\hat{z})$ is called the minimum variance direction, because the vectors vary the least along $\hat{z}$. (If $\underset{\sim}{B}$ rotated exactly in a plane, the variance of $\underset{\sim}{B}_i - \langle \underset{\sim}{B} \rangle$ along $\hat{z}$ would be zero.) The extent to which the vectors lie in a plane is measured by the ratio of intermediate to minimum eigenvalues, λ_2/λ_3; values $\gtrsim 2$ are usually taken to indicate rotation in a plane. The normal to this plane (θ_N, ϕ_N) is determined by the minimum variance analysis.

Applying the minimum variance analysis to the high-resolution data for the event in Figure 2, and plotting the magnetic field in the minimum variance coordinate system, we obtained the results shown on the right of Figure 2. There is little scatter in the z direction, consistent with the computed eigenvalue ratio $\lambda_2/\lambda_3 = 30$. The magnetic field changes mainly by rotating in the x-y plane. The normal to the x-y plane is $\theta_N = -7^\circ$, $\phi_N = 239^\circ$ in solar ecliptic coordinates.

The "thin" sector boundaries are not always isolated transitions, i.e., a SB may consist of several rapid reversals in the direction of $\underset{\sim}{B}$.

Figure 3 shows a plot of 5 min averages of B, ϕ, and θ for a 6-hr interval on January 18 and 19, 1973. A SB can be seen in the ϕ-direction at approximately hour 4 on January 19. The abrupt rise in field magnitude at $\sim$ hour 15 is at an interface to a high speed stream. The transition appears to be an isolated thin SB at this resolution, but higher resolution data (Figure 4) show that the transition actually consists of at least three abrupt reversals in $\underset{\sim}{B}$--one at $\sim$ 0418:40 UT, a second at $\sim$0422:15 UT and a third at $\sim$ 0428:40 UT. In two of the crossings (0422 and 0428 UT) the magnetic field intensity drops to near zero; i.e., these transitions are essentially null-sheets, in which the field reverses direction by shrinking to zero along a line and then increasing in the opposite direction on that line. This behavior is not discernible in the 5 min averages shown in Figure 4. This example illustrates the importance of using high resolution measurements to study the structure of SBs; it shows that even seemingly simple SBs can be relatively complex; it points out a limitation of our classification scheme; and it indicates the difficulties in trying to find a descriptive classification scheme.

Figure 5 shows an example of a second type of SB transition, which we call a "thick" SB. Hourly averages of B and θ are shown in the top panel, together with hourly averages of the proton temperature (T), density (N), and bulk speed (V). In this case the SB lasts ≈ 12 hr. Note that $\underset{\sim}{B}$ rotates out of the ecliptic and back again during the SB transition; θ is nearly 90° where ϕ appears to change by 180°. Recall that we have defined a SB as a transition of $\underset{\sim}{B}$ from one spiral direction to the opposite direction. Since $\theta \sim 0$ for a spiral direction, the sector boundary transition is defined by the variations in θ as well as in ϕ. In Figure 5, it happens that the SB is defined mainly by θ. Three additional characteristics of the SB in Figure 5 should be noted. First, the magnetic field intensity is higher inside than outside; the SB is not a null sheet. Second, a minimum variance analysis shows that $\underset{\sim}{B}$ in the sector boundary rotates through $\sim$ 180° in a plane. This is illustrated in the bottom of Figure 5. The component of $\underset{\sim}{B}$ in one direction (the minimum variance direction, here labeled z) is very small. The vector $\underset{\sim}{B}$ rotates from one sector to the other in a plane perpendicular to $\hat{z}$, i.e., the transition has the same structure as the current sheet associated with a tangential discontinuity. Third, the SB occurs just ahead of a stream at a stream interface, where T increases abruptly and N decreases (see Belcher and Davis, 1971 and Burlaga, 1974).

In some cases the SB transition is very complex. It may be difficult to identify a beginning or end; the magnetic field direction may fluctuate irregularly; and no simple patterns may be found. It is difficult to speak of the orientation or "the" internal structure of such sector boundaries. We found three "complex" SBs like this. They will be discussed separately.

Table 1 lists the 18 sector boundaries examined in this study. Eight are classified as thin, seven as thick, and 3 as complex. There is some subjectivity in this classification. For example, the thick SB on March 5, 1973 might have been classified as "complex"; and the "thin" SB on June 16, 1971, actually consists of several thin SBs. Nevertheless, our classification is useful, and it is physically meaningful.

3. Large-Scale Configurations

Consider an isolated thin or thick SB in which the magnetic field direction reverses by rotating uniformly in a plane (e.g., as in Figures 2 and 5). It is reasonable to expect that the normal to the plane of rotation is the same as the normal to the sector boundary surface. This can be verified using simultaneous observations from two suitably separated spacecraft (e.g., Helios-1, 2 or Voyager-1, 2), but in lieu of such results we shall assume it is true. A measure of planarity, λ_2/λ_3, is given in Table 1. (This cannot be determined for null sheets, in which $\underset{\sim}{B}$ varies along a line rather than in a plane.) One sees that for most thick SBs and for the isolated, thin SBs that are not null sheets, the $\underset{\sim}{B}$ vectors do lie close to a plane ($\lambda_2/\lambda_3 > 2$). Our assumption that the normal to this minimum variance plane is parallel to the SB surface normal is true only if the SB is a tangential discontinuity, i.e., only if $\underset{\sim}{B}$ is perpendicular to the surface normal. Thus, we shall consider only isolated events for which the angle (β) between the minimum variance normal and the average $\underset{\sim}{B}$ is "close" to 90°. Lepping and Behannon (1979) showed that "close" is $\gtrsim 75°$ for measurements of directional discontinuities by an instrument like that on IMP-6. Most of the thin and thick SBs in Table 1 satisfy this condition.

The normals (θ_N, ϕ_N) determined for each SB using the minimum variance method (when that was possible and meaningful) are given in Table 1. Figure 6 shows the distribution of θ_N and ϕ_N for the thin and thick SBs for the events with $\lambda_2/\lambda_3 > 2$. The ϕ distributions show that the normals tend to lie perpendicular to the spiral direction (shown by the solid arrow marked $\vec{B}$), as they must if SBs are tangential discontinuities (or resemble them, in the case of thick SBs) and if $\underset{\sim}{B}$ is along the spiral direction on each side of the TD. Thus, the ϕ distribution gives support for our assumption that the minimum variance normals are the same as the SB surface normals. It is significant that the distribution of normals is essentially the same for thin and thick SBs. Most significant, however, is the result shown by the θ distributions, viz. the minimum variance normals (and by inference, the sector boundary surface normals) lie close to the ecliptic plane. In other words, the SB surfaces are highly inclined ($\sim 40° - 90°$) with respect to the ecliptic plane.

The high inclination of the sector boundaries is related to the observations that $|\theta|$ usually reaches relatively large values in SBs and $|\underset{\sim}{B}|$ tends to be constant in the SBs that we observed. We have already noted this behavior in two examples (Figures 2 and 5). Figure 7 shows this explicitly for a thick SB. The θ and B distributions on the right were obtained from hour-averages of data inside thick SBs; the θ and B distributions on the left were obtained from hour averages outside the SBs, i.e., excluding the SB and intervals on either side of the SB roughly equal to the duration of the SB but including only data within $\pm$ 2 days of the SB. The B distributions inside the SB are essentially the same as those outside, supporting our assertion that on average B does not change appreciably inside SBs. The θ distribution inside SBs, however, differs significantly from that outside SBs. Outside, the distribution has a single peak at $\theta = 0$ and is typical of that for the solar wind in general. (This distribution together with the ϕ distribution in Figure 1 shows that the magnetic field did usually lie along the spiral direction in the sectors bordering the SBs considered in this paper.) Inside the SBs, the θ distribution is essentially bimodal, and there is a relatively high probability of finding large $|\theta|$ values. This indicates that $\underset{\sim}{B}$ often changes direction in a SB by rotating out of the ecliptic, and it is consistent with SBs being appreciably inclined with respect to the ecliptic.

Our conclusion that SB surfaces were highly inclined with respect to the ecliptic during 1971-1974 is consistent with and complements the results of Korzhov (1978). Using OSO-7 observations of the white-light corona to determine the configuration of coronal streamers and thereby infer the orientation of the sector boundary surfaces between 3-10 R_o, he showed that the SBs of May 12, May 27, and June 10, 1973, were highly inclined with respect to the solar equator near the sun (Figure 8a). Our results (Table 1) show that the same SBs were highly inclined with respect to the ecliptic (θ_N = 20°, 36°, -15°, respectively) near 1 AU. Our results are also consistent with the general orientations of near-sun sector boundaries computed from photophere magnetic field measurements for the period November 3, 1973-February 16, 1974 (Burlaga et al., 1978).

The conclusion that the SB surfaces were highly inclined to the ecliptic might appear to conflict with the result of Smith et al. (1978) that SBs are confined to $\lesssim$ 16° latitude and with the result of Villante et al. (1979) that the SB surface was approximately a sinusoid with an amplitude in latitude of $\lesssim$ 10°. Note, however, that their results were obtained in 1976 near solar minimum, whereas our results refer to the period 1971 through 1973, near solar maximum and during the decline in solar activity. In the latter period, it is known that there were large equatorial coronal holes, and Burlaga et al. (1978) have shown how closely spaced equatorial coronal holes can lead to highly inclined SB surfaces. By contrast, in the former period (1976) there were presumably few if any large equatorial holes (Nolte et al., 1977) and the flows may have originated at higher latitudes, giving a near-equatorial SB with a small inclination to the ecliptic most of the time. Thus, there may be a solar cycle variation in the inclination of SB surfaces, as suggested schematically in Figure 8. Our results suggest such a relation, but they do not prove it. It is important to carry out an analysis similar to ours for SBs observed near solar minimum.

4. Directional Discontinuities in and near SBs

It is well known that the interplanetary magnetic field is "discontinuous", i.e., a stationary observer finds that approximately once or twice per hour the direction of $\underset{\sim}{B}$ changes by $\gtrsim 30°$ in $\lesssim 30$ sec. (Ness et al., 1966; Burlaga and Ness, 1968; Burlaga, 1969; Siscoe et al., 1968). Many of these directional discontinuities are tangential discontinuities (see Burlaga et al., 1977 and the references therein). We have found that directional discontinuities are present inside thick SBs and outside near all types of SB. Since tangential discontinuities are current sheets one might ask whether the orientations of current sheets in and near SBs are related to the orientations of SB surfaces. If this were so, one would have an additional tool for studying the morphology of SBs.

We identified directional discontinuities by inspection of 1-hr plots of 15s averages of B, θ, ϕ for the 4-day intervals containing the SBs listed in Table 1. Approximately 700 discontinuities were selected from $\lesssim$ 900 hrs of data. Each of these was analyzed using the minimum variance analysis described above. In order to select the tangential discontinuities, we considered only events for which 1) $\lambda_2/\lambda_3 \geq 2.0$, 2) the change in magnetic field direction (ω) was $\geq 60°$ (Fitzenreiter, private communication, showed that the condition $\omega \gtrsim 30°$ used in most previous studies can lead to mistakes in identifying rotational discontinuities, because of certain systematic errors), and 3) the angle (ρ) between the minimum variance direction and the average field vector was $\gtrsim 75°$ (Lepping and Behannon, 1979).

Table 2 shows statistics describing the tangential discontinuities that we selected in and near SBs. The rate of directional discontinuities was $\lesssim$ 1/hr, consistent with previous results. Only a fraction of these (15%) were selected for studies of morphology, because of our conservative definition of a tangential discontinuity. There are two significant new results in Table 2: 1) The rate of these tangential discontinuities inside thick SB is essentially the same as that outside, and 2) The rate of tangential discontinuities with $\omega > 120°$ is significantly higher inside SBs than outside; these are not themselves SBs, since they mark no clear change from one sector polarity to another.

The normals which were determined for the tangential discontinuities by the minimum variance analysis should be accurate to within several degrees. The distributions of θ_N and ϕ_N for these normals are shown in Figure 9. As expected, the distributions for tangential discontinuities outside the SBs closely resemble those published previously (Burlaga, 1969; Siscoe et al., 1968); the normals tend to be perpendicular to the spiral direction and at latitudes between ±45°. The θ_N, ϕ_N distributions for tangential discontinuties inside thick sector boundaries are found to closely resemble those outside SBs. In particular, the average directions and the range of directions of normals inside SBs are similar to those of normals outside. Inspection of normals in individual SBs shows that the scatter of normal directions is large in almost every case. Thus, the results in Figure 9 are not due to a coincidence in the orientations of SBs, but rather to the fact that discontinuities inside SBs have the same statistical orientations as those outside. We conclude that tangential discontinuities among the directional discontinuities in thick SBs cannot generally be used to determine the orientations of SBs.

5. Magnetic Holes in and near Sector Boundaries

Although we have shown that most SBs are not null sheets, it is nevertheless true that null sheets may often be found in SBs. In the following discussion, we shall include current sheets in which the magnetic field drops to low but non-zero values. These are called magnetic holes (Turner et al., 1977). An example of a thick SB containing magnetic holes in shown in Figure 10.

Magnetic holes pass Earth at the rate of $\sim$ 1 to 2 per day (Turner et al., 1977). We found a similar rate (0.06/hr or 1.4/day) for 15 hour intervals adjacent to the thick SBs which we selected. Inside the thick SBs, however, the rate was significantly higher--0.15/hr or 3.6/day. The absolute rates for holes inside and outside SBs depend on our subjective selection procedure, but the relative rate (inside to outside), which is the most significant number, is not sensitive to the selection procedure. Considering that SBs occur in low-speed flows, the ratio of the spatial "density" of magnetic holes inside SBs to that outside is $\gtrsim$ 0.15/0.06 = 2.5. A preponderance of magnetic dips in SBs was also noted by Behannon and Neubauer (1979).

The rate at which magnetic holes are observed in and near thick and thin SBs, depends on the distance from the sector boundary. This is shown in Figure 11 where the number of magnetic holes in successive 3-hr intervals is plotted as a function of the time before and after the passage of the center of a SB for our set of SBs. Clearly, most magnetic holes occur between 0 to 12 hrs after the passage of the center of a SB.

Sector boundaries usually occur 0-12 hr ahead of stream interfaces when interfaces are present. This is shown in Figure 11a, where the time of the stream interface relative to the time of the center of the sector boundary is shown by the vertical lines on the abcissa. We have plotted the rate of magnetic holes with respect to the time of the stream interface (Figure 11b) for 15 hrs before and after each interface. Here one sees a clear peak at the time of passage of the stream interface, suggesting that the holes are more closely related to the interfaces than to the centers of SBs. An interface represents the transition between two flows. The magnetic holes near interfaces could be due to material trapped between the adjacent converging flows near the sun, or they might be due to some instability at the interface.

6. Summary

We have examined the orientations of sector boundaries (SBs) observed by IMP-6 between January 1971-January 1974, choosing only those cases with relatively complete sets of plasma and magnetic field data within ±2 days of the SB. It was found that the durations of the SBs were either relatively short ($\lesssim$ 10 min) or relatively long ($\gtrsim$ 3 hr); hence we classified them as "thin" and "thick". We distinguished relatively simple boundaries (in which there was a well-defined minimum variance direction) from complex boundaries. It was assumed that if the magnetic field changed direction by rotating in a plane with a negligible component of $\underset{\sim}{B}$ normal to the plane, then that plane was parallel to the surface of the SB. Using the minimum variance technique, it was found that the sector boundary surfaces were inclined appreciably with respect to the ecliptic at this epoch of the solar cycle (1971-1973). However, it was suggested that this might be due to the presence of near-equatorial coronal holes, and it was noted that the inclinations of the sector boundary surfaces might be different at another epoch, when there are no near-equatorial coronal holes.

We examined the orientations of tangential discontinuities among directional discontinuities near all SBs, and inside thick SBs, considering the possibility that they might be related to the orientations of the SBs. However, the distributions of their normals were very simila. to the corresponding distributions for tangential discontinuities located away from SBs.

Magnetic holes were found in and near sector boundaries at a higher than average rate. This appears to be related to the proximity of magnetic holes to stream interface and converging flows rather than simply to the SBs themselves.

REFERENCES

Alfvén, H. Electric currents in cosmic plasmas, Rev. Geophys. Space Phys., 15, 271, 1977.

Behannon, K. W. and F. M. Neubauer, Innvestigation of sector boundar fine structure between 0.3 and 1 AU, Solar Wind 4, ed. H. R. Rosenbauer, Springer-Verlag, to be published, 1979.

Behannon, K. W., F. M. Neubauer, and H. Barnstorf, Fine-scale characteristics of interplanetary sector boundaries, in preparation, 1979.

Belcher, J. W. and L. Davis, Jr., Large amplitude Alfvén waves in the interplanetary medium, 2., J. Geophys. Res., 76, 3534, 1971.

Burlaga, L. F., Directional discontinuities in the interplanetary magnetic field, Solar Phys., 7, 72, 1969.

Burlaga, L. F., Interplanetary stream interfaces, J. Geophys. Res., 79, 3717, 1974.

Burlaga, L. F., K. W. Behannon, S. F. Hansen, G. W. Pneuman, and W. C. Feldman, Sources of magnetic fields in recurrent interplanetary streams, J. Geophys. Res., 83, 4177, 1978.

Burlaga, L. F., J. F. Lemaire, and J. M. Turner, Interplanetary current sheets at 1 AU, J. Geophys. Res., 82, 3191, 1977.

Burlaga, L. F. and N. F. Ness, Macro and microstructure of the interplanetary magnetic field, Canadian J. of Physics, 46, S962, 1968.

Fairfield, D. H., Whistler waves observed upstream from collisionless shocks, J. Geophys. Res., 79, 1368, 1974.

Fairfield, D.H., and N. F. Ness, Interplanetary sector structure: 1970-1972, J. Geophys. Res., 79, 5089, 1974.

Hundhausen, A. J., Coronal Expansion and Solar Wind, Springer-Verlag, New York, 1972.

Hundhausen, A. J., An interplanetary view of coronal holes in Coronal Holes and High Speed Wind Streams, p. 225, J. B. Zirker, ed., Colorado Associated University Press, 1977.

King, J. H., Interplanetary Medium Data Book, NSSPC/WPC-A, R&S, 77-04, 1977.

Korzhov, N. P., The three-dimensional structure of the interplanetary magnetic field, Soviet Astron., 22, 53, 1978.

Lepping, R. P. and K. W. Behannon, Magnetic field directional discontinuities: 1. Minimum variance errors, to appear in J. Geophys. Res., 1979.

Levy, E. H., The interplanetary magnetic field structure, Nature, 261, 394, 1976.

Ness, N. F., C. S. Scearce, and S. Cantarano, Preliminary results from the Pioneer 6 magnetic field experiment, J. Geophys. Res., 71, 3305, 1966.

Nolte, J. T., J. M. Davis, M. Gerassimenko, A. J. Lazarus, and J. Sullivan, A comparison of solar wind streams and coronal structure near solar minimum, Geophys. Res. Lett., 4, 291, 1977.

Rosenberg, R. L., Latitude dependence of IMF dominant polarity, J. Geophys. Res., 10, 1339, 1975.

Rosenberg, R. L., Unified theory of the interplanetary magnetic field, Solar Phys., 15, 72, 1970.

Rosenberg, R. L. and P. J. Coleman, Heliographic latitude dependence of the dominant polarity of the interplanetary magnetic field, J. Geophys. Res., 74, 5611, 1969.

Schulz, M. Interplanetary sector structure and the heliomagnetic equator, Astrophys. and Space. Sci., 24, 371, 1973.

Siscoe, G., L. Davis, Jr., P. J. Coleman, Jr., E. J. Smith, and D. E. Jones, Power spectra and discontinuities of the interplanetary magnetic field: Mariner 4, J. Geophys. Res., 73, 61, 1968.

Smith, E. J., B. T. Tsurutani, R. L. Rosenberg, Observations of the interplanetary sector structure up to heliographic latitudes of 16°. Pioneer 11, J. Geophys. Res., 83, 717, 1978.

Sonnerup, B. U. O. and L. J. Cahill, Magnetopause structure and attitude from Explorer 12 observations, J. Geophys. Res., 72, 171, 1967.

Svalgaard L., Evidence for sun-weather relations, in Physics of Solar Planetary Environments, p. 1012, D. J. Williams, ed., published by American Geophysical Union, 1976.

Svalgaard, L., J. M. Wilcox, and T. L. Duvall, A model combining the polar and sector structured magnetic fields, Solar Phys., 38, 151, 1974.

Turner, J. M., L. F. Burlaga, J. F. Lemaire, and N. F. Ness, Magnetic holes in the solar wind, J. Geophys. Res., 82, 1921, 1977.

Villante, U., R. Bruno, F. Mariani, L. F. Burlaga, and N. F. Ness, The shape and location of the sector boundary surface in the inner solar system, J. Geophys. Res., in press, 1979.

Wilcox, J. M., The interplanetary magnetic field. Solar origin and terrestrial effects, Space Sci. Rev., 8, 258, 1968.

Wilcox, J. M., P. H. Scherrer, L. Svalgaard, W. O. Roberts, R. H. Olson and R. L. Jenne, Influence of solar magnetic sector structure on terrestrial atmospheric vorticity, J. Atmos. Sci., 31, 581, 1974.

Wilcox, J. M. and N. F. Ness, Quasi-stationary corotating structure in the interplanetary medium, J. Geophys. Res., 70, 5793, 1965.

Wilcox, J. M. and L. Svalgaard, Coronal magnetic structure at a solar sector boundary, Solar Phys., 34, 461, 1974.

TABLE 1

IMP-6 Sector Boundaries (1971-1973)

Class	Year	Dec. Day	λ_2/λ_3	β(deg.)	ω(deg.)	θ_N	ϕ_N	Remarks
	1971	87	3.1	37	126	24	221	RD
	1971	166	40	89	159	-37	216	Multiple
	1973	5	30	86	175	-7	239	
	1973	17	8.0, 8.1, 5.9	78, 80, 89	162, 167, 141	-8, 37, 34	190, 191, 213	Multiple
Thin	1973	131	16.2	85	150	20	125	
	1973	146	14.1	77	179	36	217	
	1974	13	-	-	-	-	-	Holes
	1974	23	-	-	-	-	-	Holes
	1971	97	3.2	46	116	-32	180	
	1972	40	15.2	50	122	34	212	
	1972	63	3.7	56	144	13	194	
Thick	1972	76	2.7	51	131	14	241	
	1972	74	7.7	79	127	-6.4	229	
	1972	100	5.2	107	154	30	201	
	1973	90	13.6	95	136	-1	181	
Complex	1971	124	3.5	95	108	-36	222	
	1972	93	-	-	-	-	-	Holes
	1973	160	7.1	74	141	-15	238	

TABLE 2

Directional Discontinuities at SBs

	Number	Number/hr
Directional Discontinuities	758	0.92
Events with $\lambda_2/\lambda_3 \geq 2$ and $\omega \geq 60°$	250	0.39
TDs ($\beta > 75°$)	129	0.14
TDs in SBs	27	0.21
TDs outside SBs	107	0.15
TDs with $\omega > 120°$ in SBs	14	0.18
TDs with $\omega > 120°$ outside SBs	30	0.04

FIGURE CAPTIONS

FIGURE 1 Distributions of hour averages of ϕ, B and σ before and after the sector boundaries considered in this study.

FIGURE 2 Observations of a thin sector boundary. Also shown are the variations of $\underset{\sim}{B}$ in the B_x-B_y plane (normal to the minimum variance direction B_z) and in the B_z-B_y plane.

FIGURE 3 Example of a thin sector boundary with structure that is unresolved in the averages shown here (see Figure 4).

FIGURE 4 Discontinuities observed in high resolution data for the sector boundary shown in Figure 3.

FIGURE 5 Example of a thick sector boundary. The SB occurs ahead of an interface in front of a high speed stream. The field changes direction by rotating in a plane through large $|\theta|$ angles.

FIGURE 6 Distributions of θ_N and ϕ_N for normals to thick and thin sector boundaries. The normals tend to be perpendicular to the spiral direction and close to the ecliptic in 1971-1973.

FIGURE 7 Distributions of hour averages of θ and B inside and outside of the thick SB. The θ angles tend to be larger inside SB than outside, while the magnitude remain near the average value for the solar wind, indicating that $\underset{\sim}{B}$ tends to change direction in SBs by rotating out of the ecliptic.

FIGURE 8 An illustration of a possible solar cycle dependence of the orientation at the SB surface. a) Results after Korzhov (1978) showing high inclinations with respect to the solar equatorial plane in 1973. b) Results after Villante et al. (1979) showing low inclinations in 1976.

FIGURE 9 Distributions of the directions of normals to tangential discontinuities at SBs and away from SBs.

FIGURE 10 Example of a magnetic hole in a sector boundary.

FIGURE 11 a) Distribution of magnetic holes relative to the centers of the sector boundaries for the cases when stream interfaces (IF) were present. The positions of the interfaces relative to the centers of the sector boundaries are shown. b) Distribution of magnetic holes relative to stream interfaces. This figure shows that magnetic holes are predominant near stream interfaces.

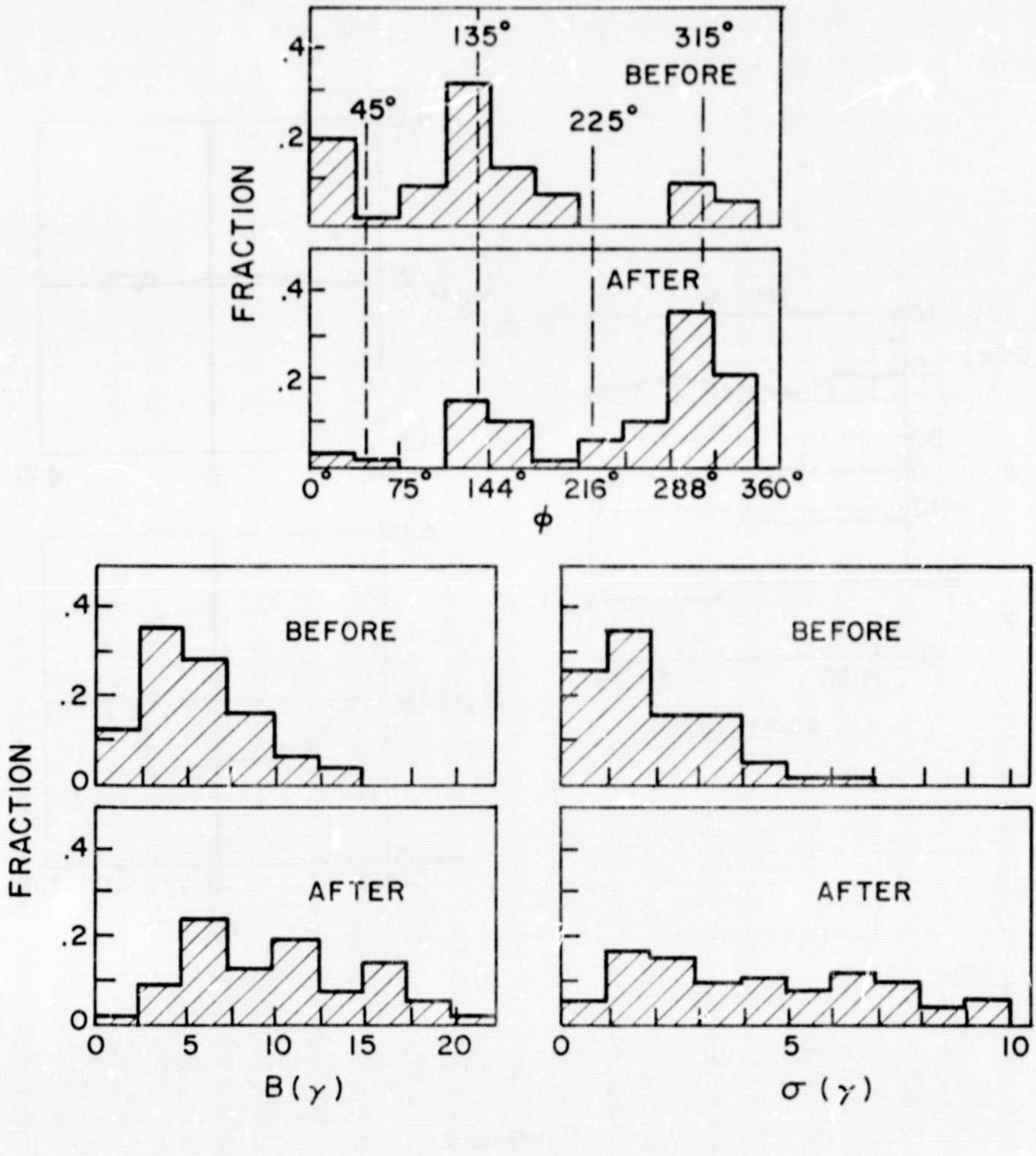

FRACTION
.4
.2
135°
315°
BEFORE
45°
225°
AFTER
0°
75°
144°
216°
288°
360°
ϕ
.4
.2
0
BEFORE
AFTER
0
5
10
15
20
$B(\gamma)$
0
5
10
$\sigma(\gamma)$

Figure 1

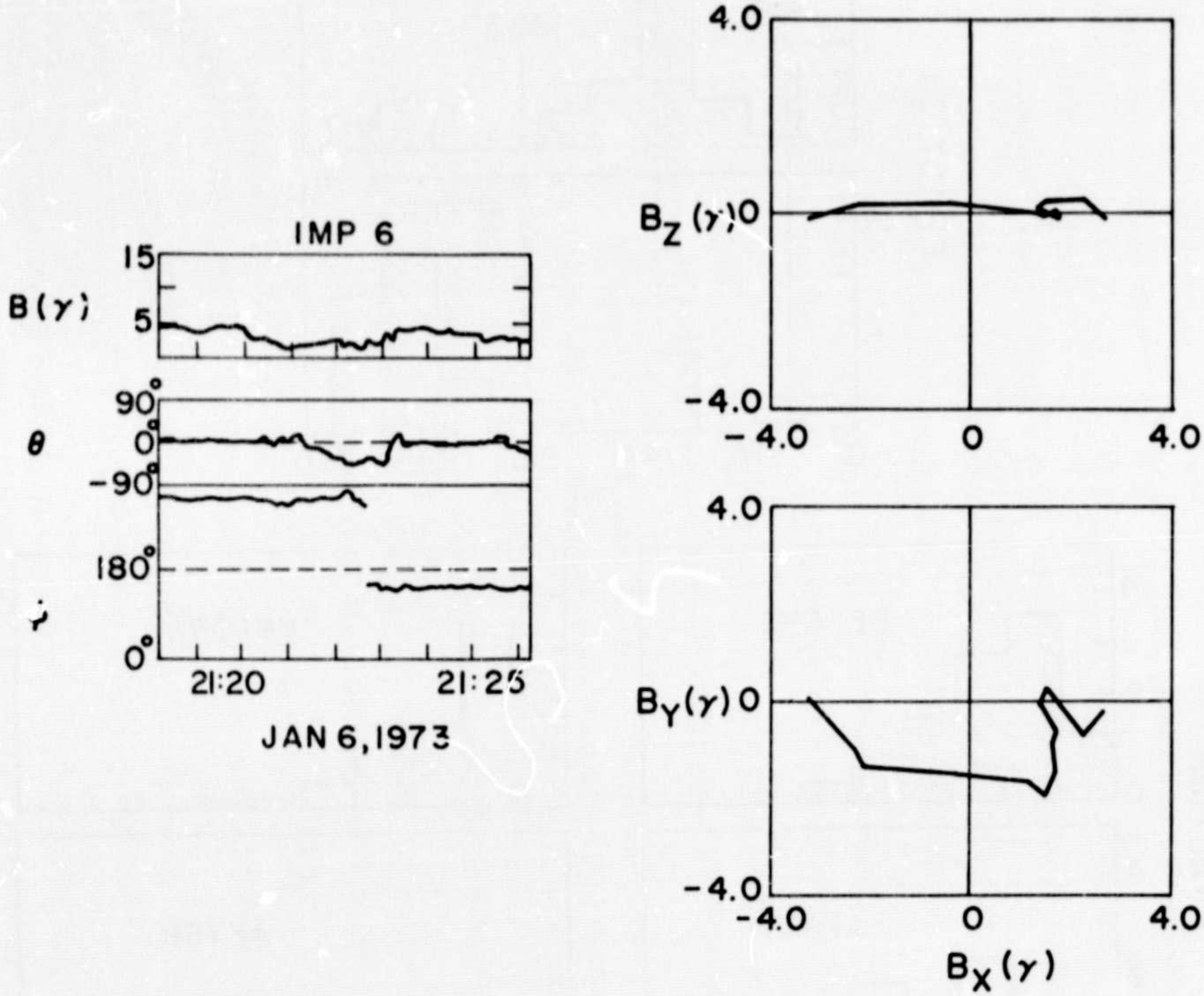

IMP 6
B(γ)
15
5
90°
θ
0°
-90°
180°
φ
0°
21:20
21:25
JAN 6, 1973
4.0
$B_Z (\gamma)$ 0
-4.0
-4.0
0
4.0
4.0
$B_Y (\gamma)$ 0
-4.0
-4.0
0
4.0
$B_X (\gamma)$

Figure 2

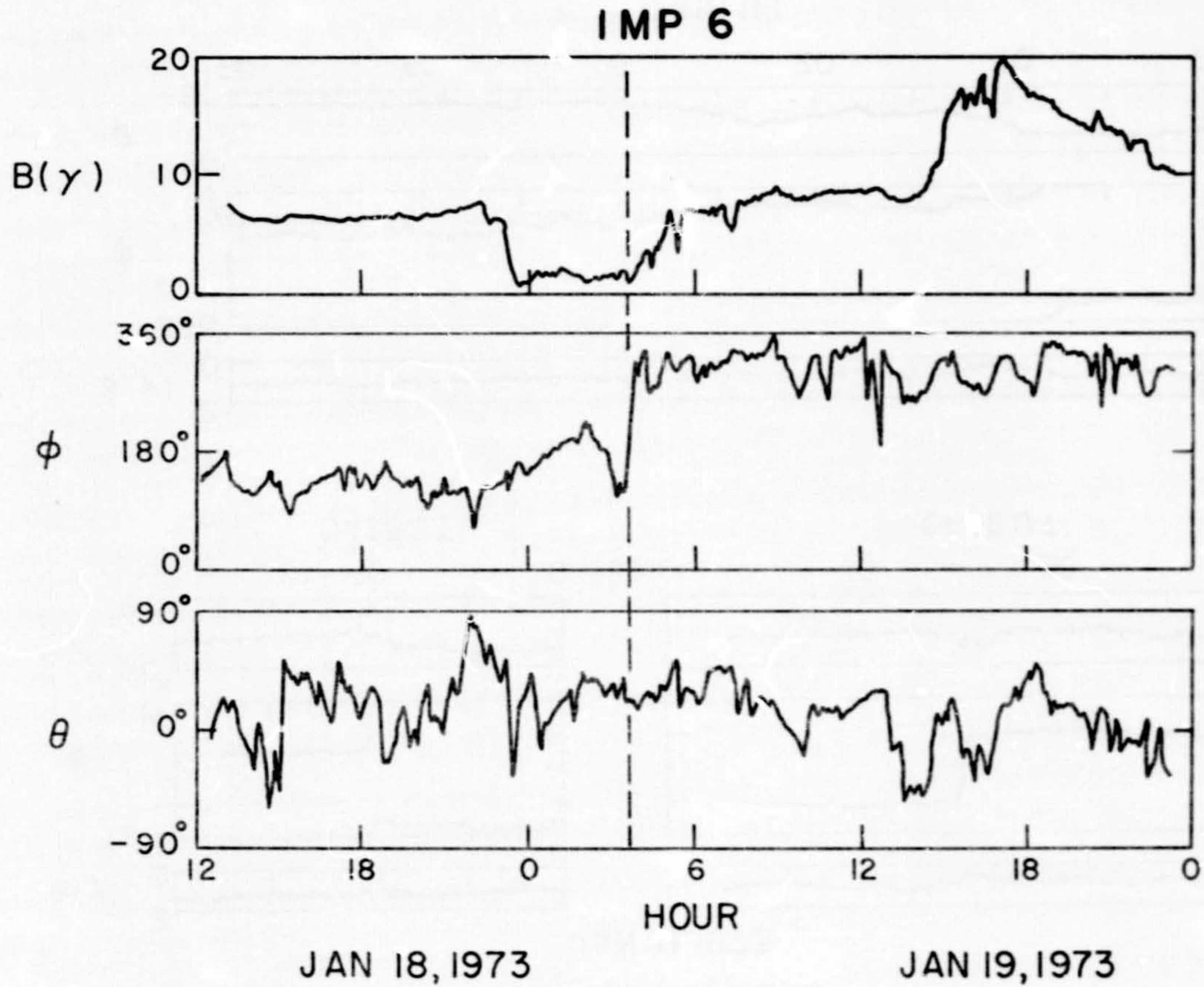
IMP 6
B(γ)
20
10
0
φ
360°
180°
0°
θ
90°
0°
-90°
12
18
0
6
12
18
0
HOUR
JAN 18, 1973
JAN 19, 1973

Figure 3

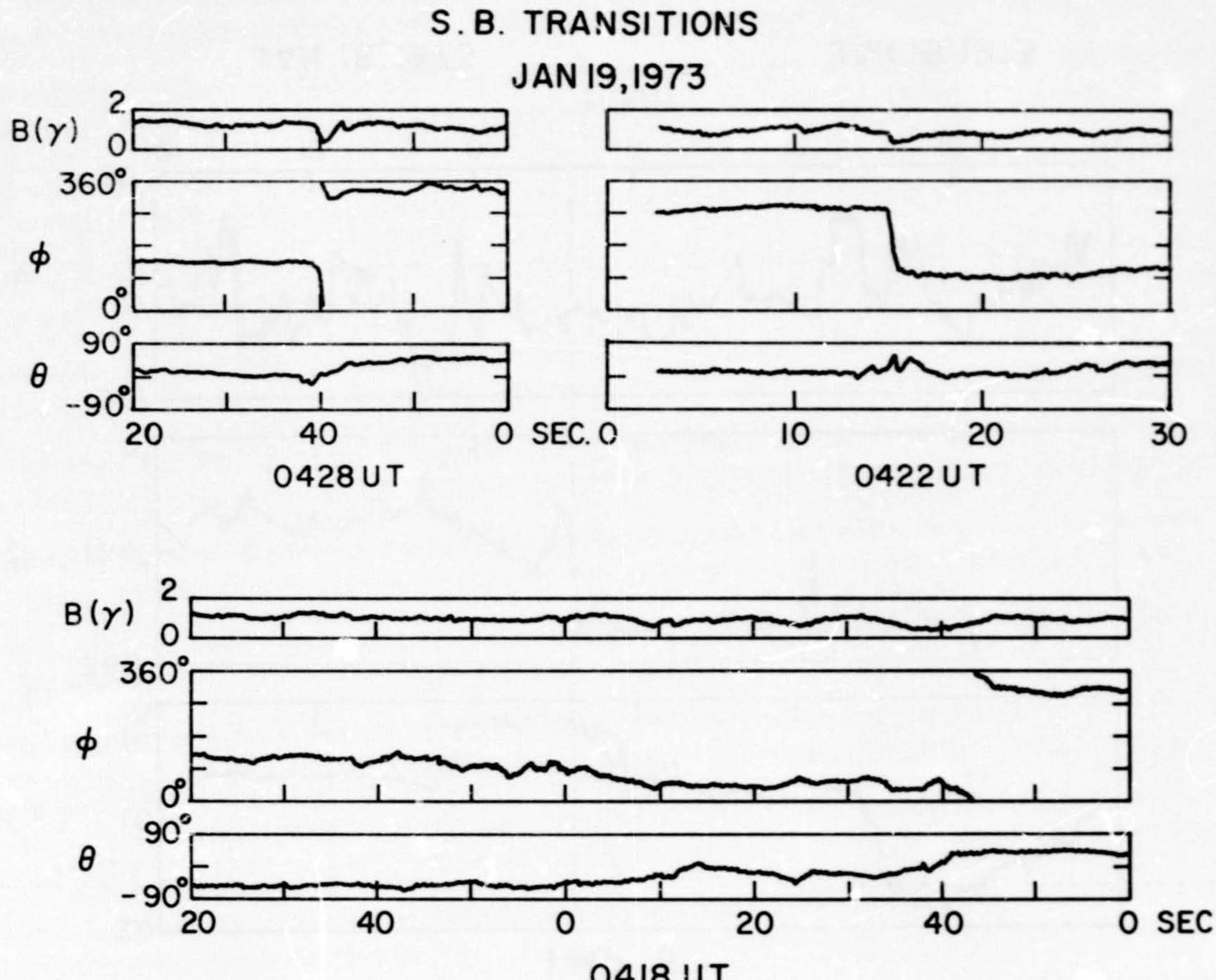
S. B. TRANSITIONS
JAN 19, 1973
B(γ)
2
0
φ
360°
0°
θ
90°
-90°
20
40
0 SEC. 0
10
20
30
0428 UT
0422 UT
40
0
0 SEC
0418 UT

Figure 4

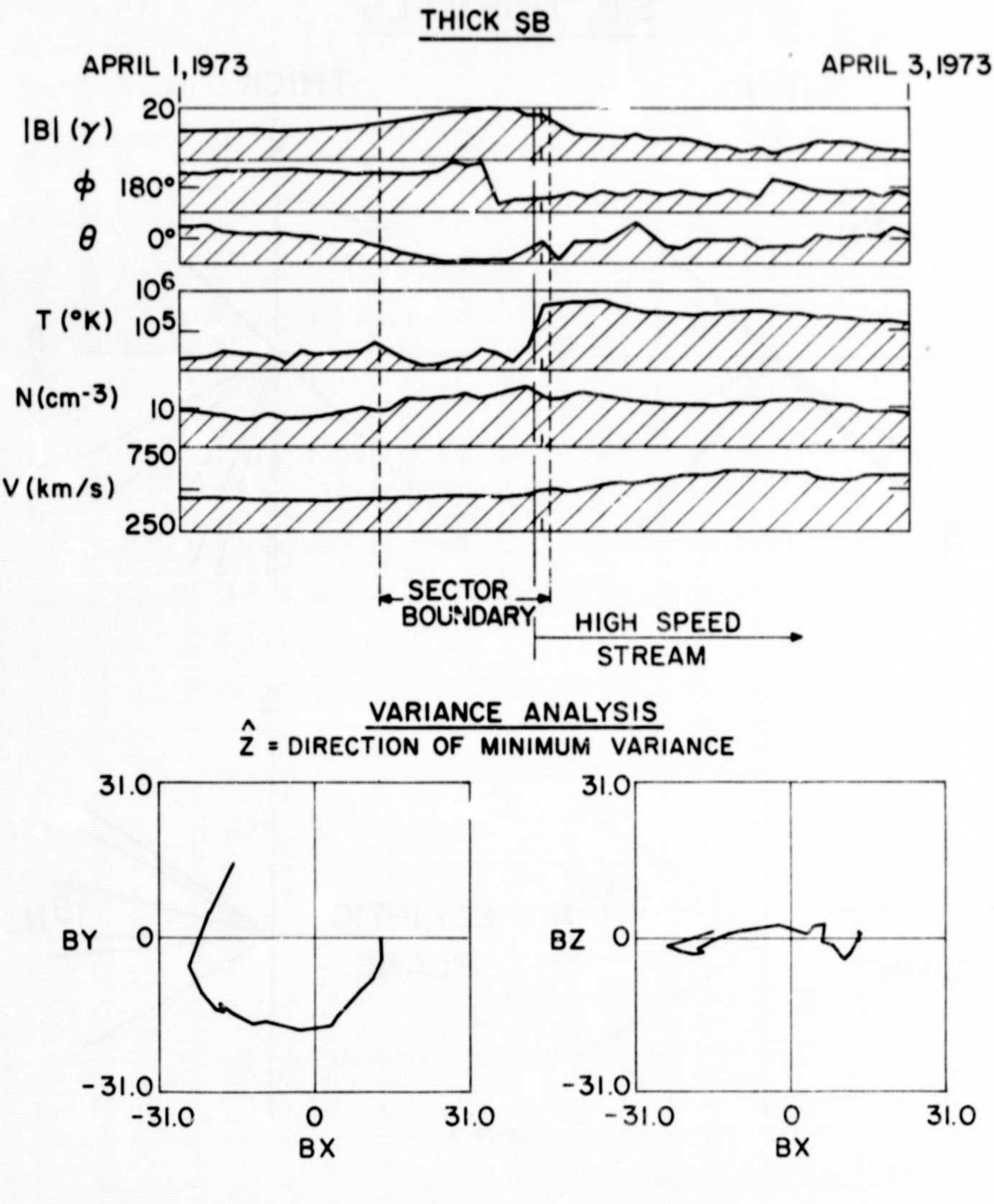
THICK SB
APRIL 1, 1973
APRIL 3, 1973
|B| (γ)
20
φ
180°
θ
0°
T (°K)
10⁶
10⁵
N(cm⁻³)
10
V (km/s)
750
250
SECTOR
BOUNDARY
HIGH SPEED
STREAM
VARIANCE ANALYSIS
Ẑ = DIRECTION OF MINIMUM VARIANCE
31.0
BY
0
-31.0
-31.0
0
31.0
BX
31.0
BZ
0
-31.0
-31.0
0
31.0
BX

Figure 5

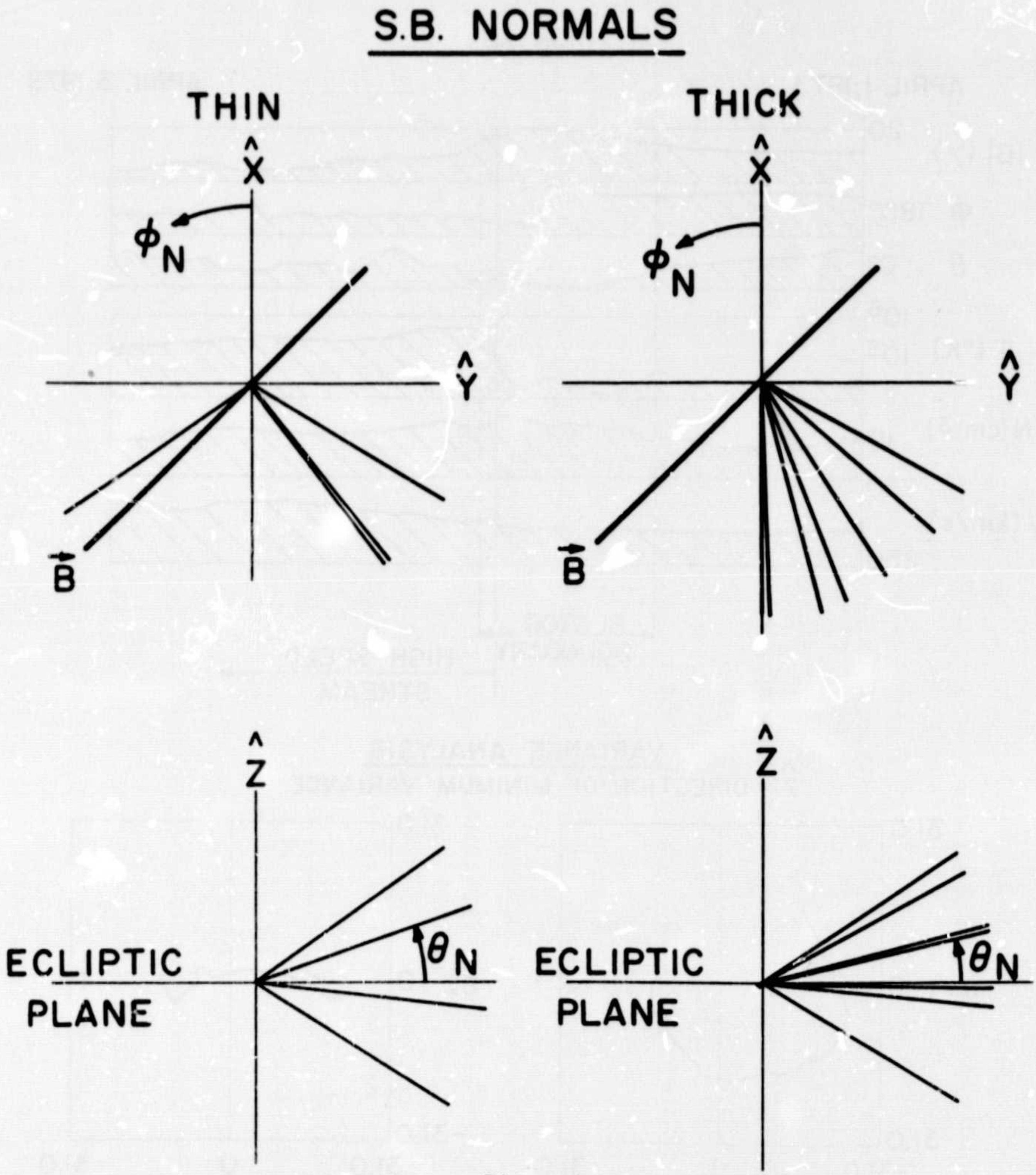
S.B. NORMALS
THIN
THICK
$\hat{X}$
ϕ_N
$\hat{Y}$
$\vec{B}$
$\hat{X}$
ϕ_N
$\hat{Y}$
$\vec{B}$
$\hat{Z}$
θ_N
ECLIPTIC
PLANE
$\hat{Z}$
θ_N
ECLIPTIC
PLANE

Figure 6

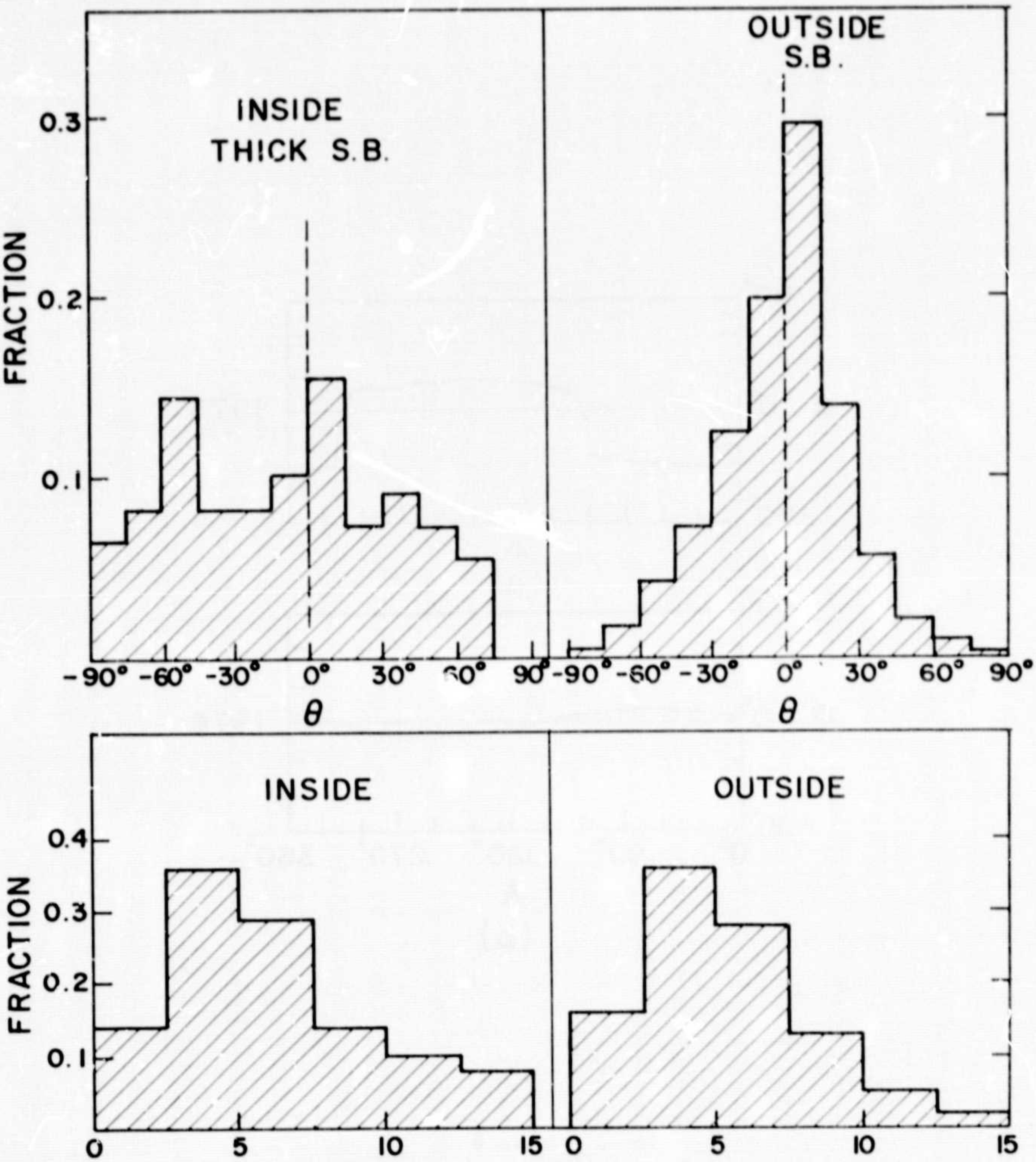
INSIDE
THICK S.B.
OUTSIDE
S.B.
FRACTION
0.3
0.2
0.1
-90° -60° -30° 0° 30° 60° 90°
-90° -60° -30° 0° 30° 60° 90°
θ
θ
INSIDE
OUTSIDE
FRACTION
0.4
0.3
0.2
0.1
0 5 10 15
0 5 10 15
B(γ)
B(γ)

Figure 7

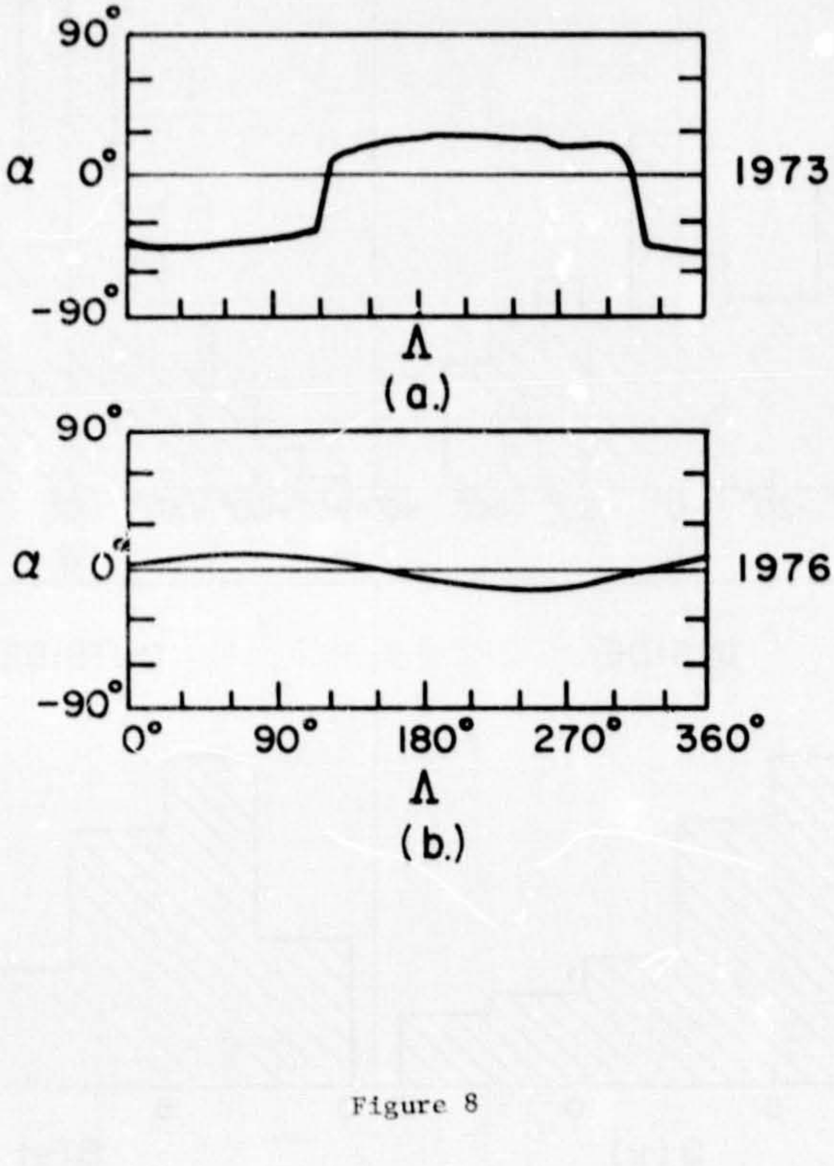

Figure 8

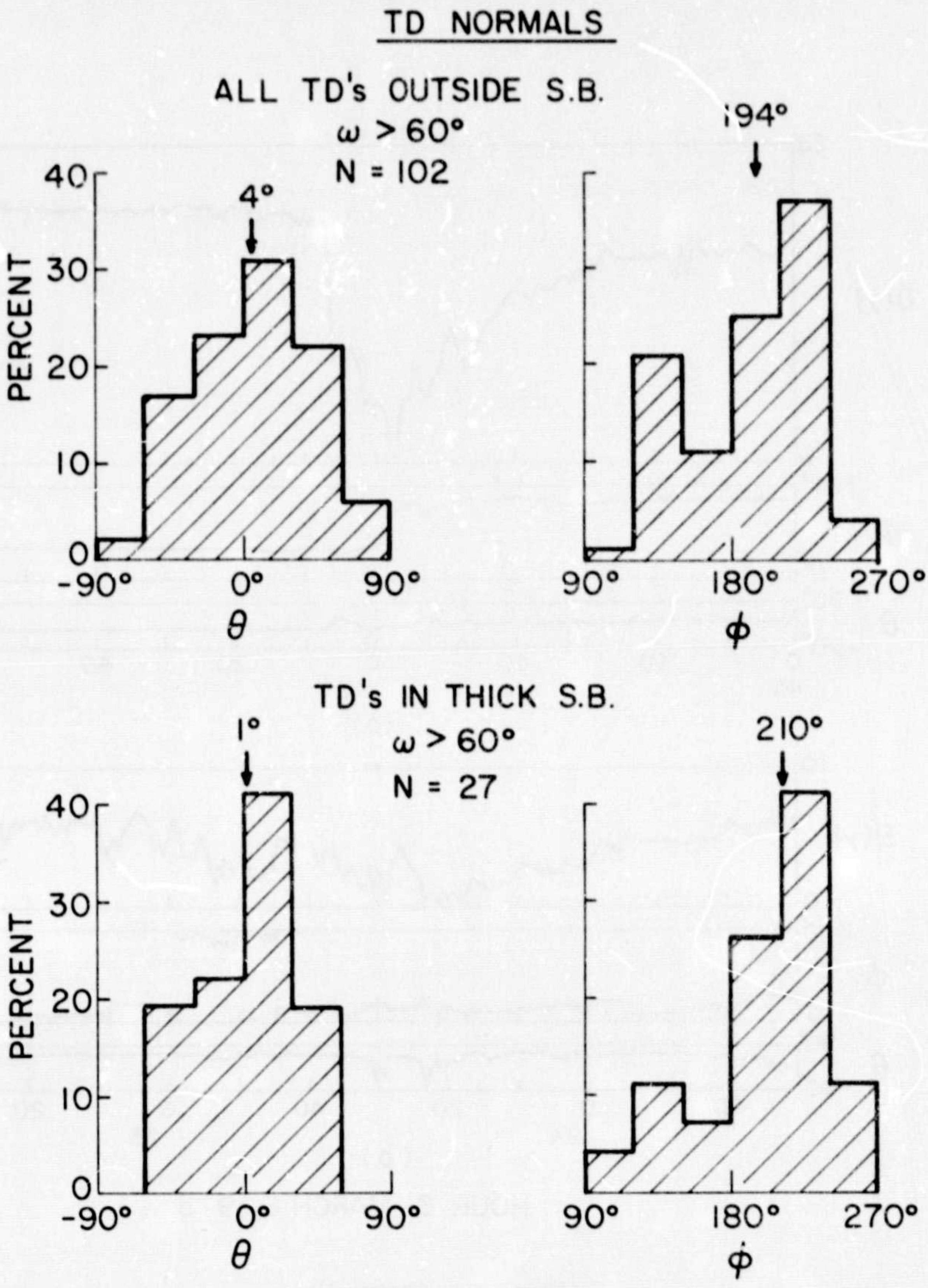
TD NORMALS
ALL TD's OUTSIDE S.B.
ω > 60°
N = 102
4°
194°
PERCENT
40
30
20
10
0
-90°
0°
90°
θ
90°
180°
270°
φ
TD's IN THICK S.B.
ω > 60°
N = 27
1°
210°
PERCENT
40
30
20
10
0
-90°
0°
90°
θ
90°
180°
270°
φ

Figure 9

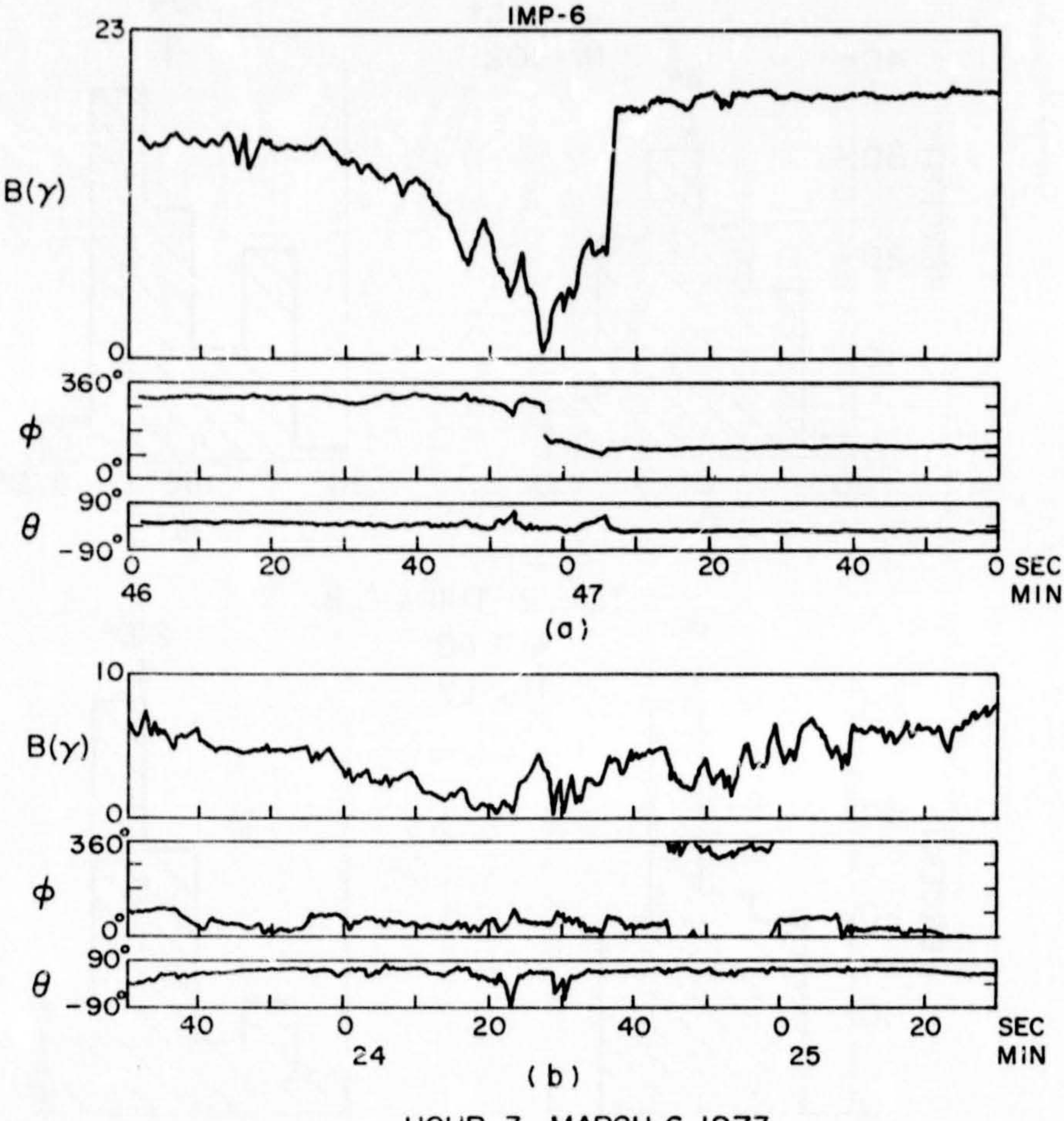

IMP-6
23
B(γ)
0
360°
φ
0°
90°
θ
-90°
0
20
40
0
20
40
0 SEC
46
47
MIN
(a)
10
B(γ)
0
360°
φ
0°
90°
θ
-90°
40
0
20
40
0
20
SEC
24
25
MIN
(b)
HOUR 3, MARCH 6, 1973

Figure 10

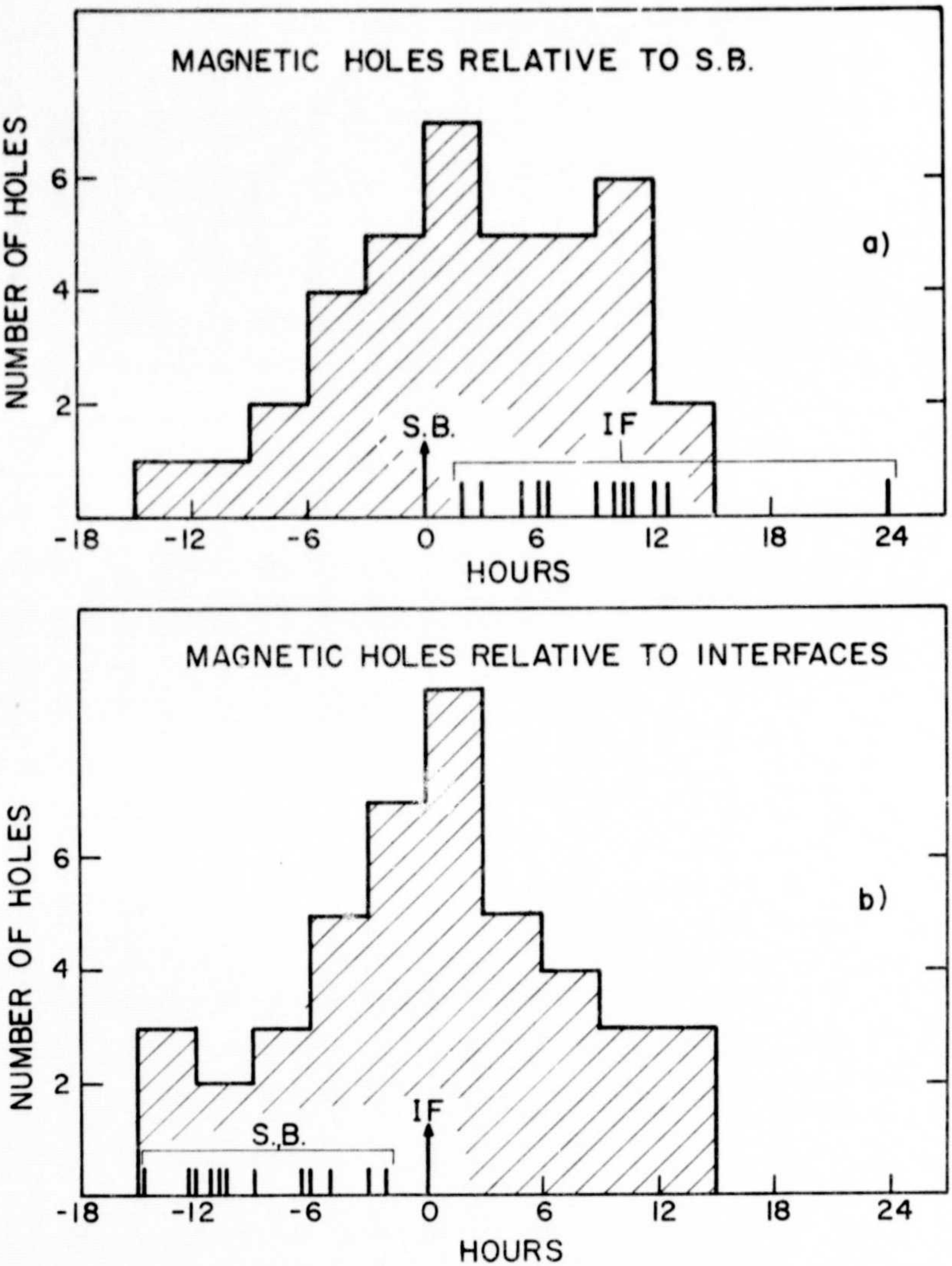
MAGNETIC HOLES RELATIVE TO S.B.
NUMBER OF HOLES
6
4
2
a)
S.B.
IF
-18
-12
-6
0
6
12
18
24
HOURS
MAGNETIC HOLES RELATIVE TO INTERFACES
NUMBER OF HOLES
6
4
2
b)
S.B.
IF
-18
-12
-6
0
6
12
18
24
HOURS

Figure 11